Built-in anionic equilibrium for atom-economic recycling of spent lithium-ion batteries

Pengfei Zhu[a], Zhipeng Jiang[a], Wei Sun[b], Yue Yang[b], Debbie S. Silvester[c], Hongshuai Hou[a], Craig E. Banks[d], Jiugang Hu*[a], Xiaobo Ji*[a]

[a] College of Chemistry and Chemical Engineering, Central South University, Changsha 410083, China.

[b] School of Minerals Processing and Bioengineering, Central South University, Changsha 410083, China.

[c] School of Molecular and Life Sciences, Curtin University, GPO Box U1987, Perth, Western Australia 6845, Australia.

[d] Faculty of Science and Engineering, Manchester Metropolitan University, Chester Street, Manchester M1 5GD, UK.

Corresponding authors: fax: +86-731-88879616

E-mail: hujiugang@csu.edu.cn; xji@csu.edu.cn

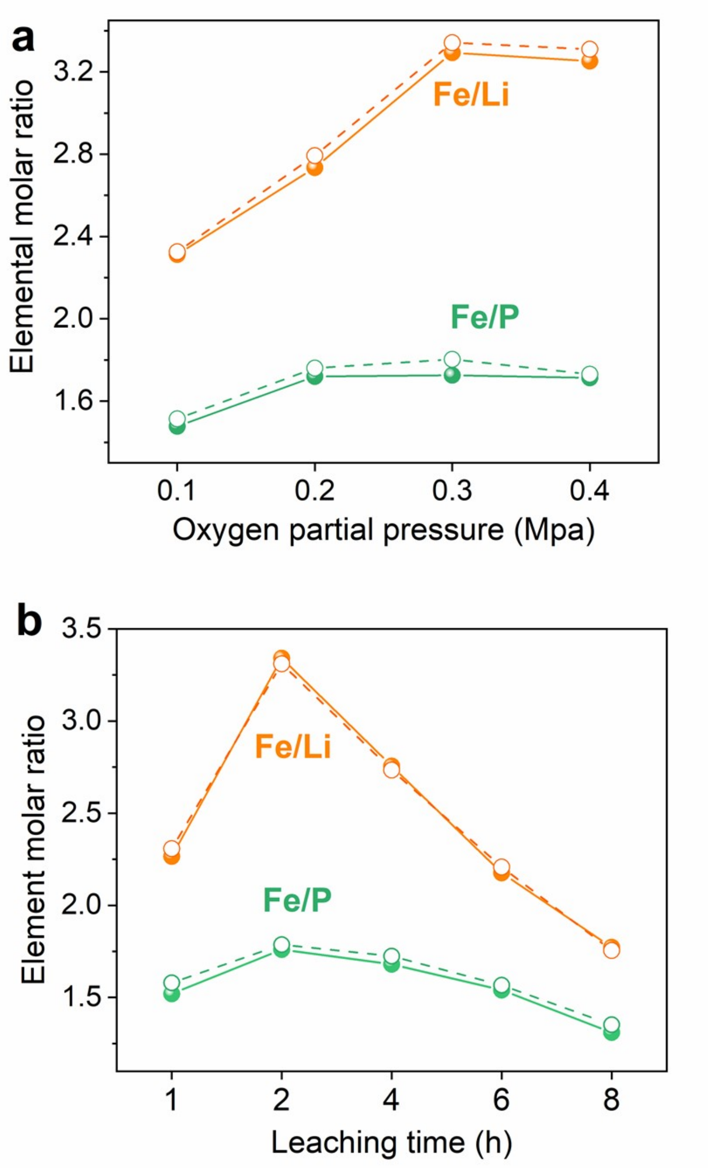

Figure S1. Elemental molar ratios of Fe/Li, Fe/P in the leaching residues under (a) various oxygen partial pressures and (b) leaching time. (Solid line and filled dots represent the measured values, dashed line and hollow dots represent the theoretical values).

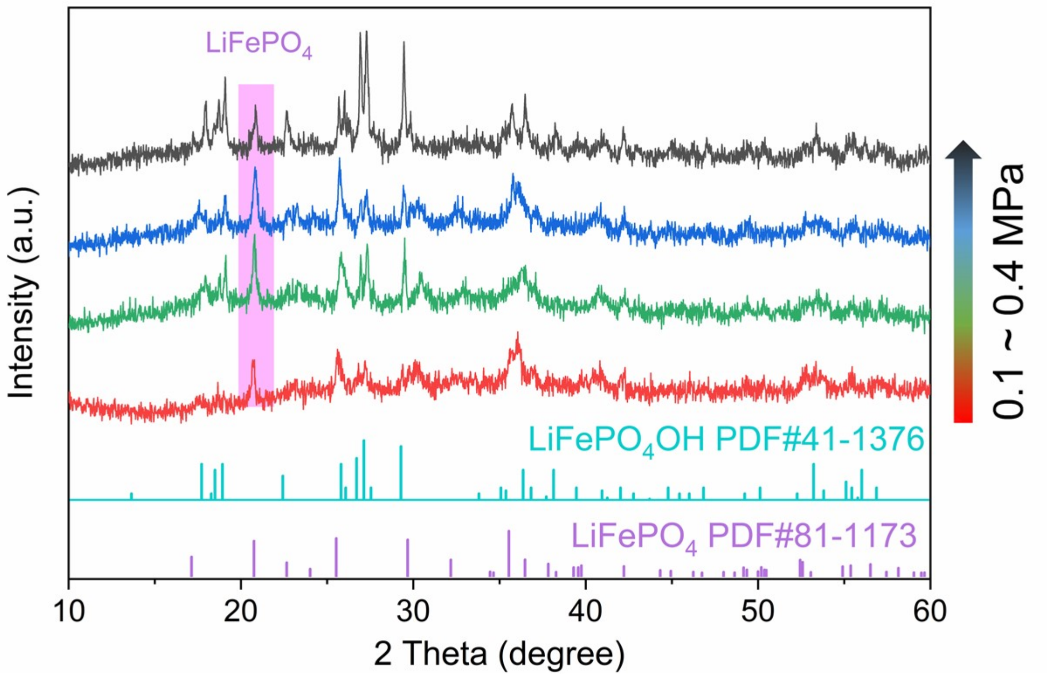

Figure S2. XRD patterns of leaching residues under various oxygen partial pressures. (Temperature: 210 °C; leaching time: 2 h).

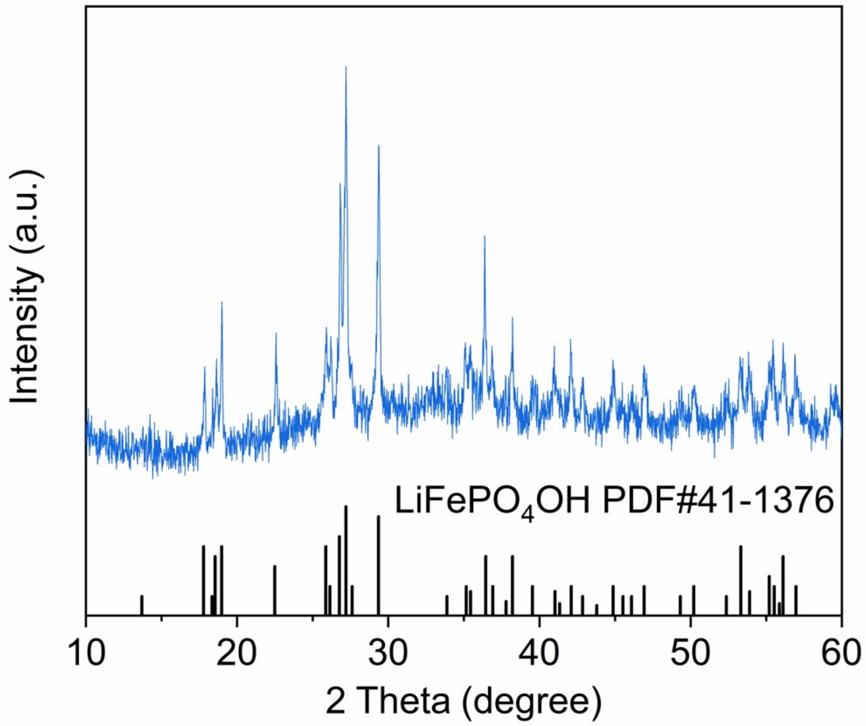

Figure S3. XRD pattern of leaching residue with 8 h’ leaching time. (Temperature: 210 °C; Partial oxygen pressure: 0.3 MPa).

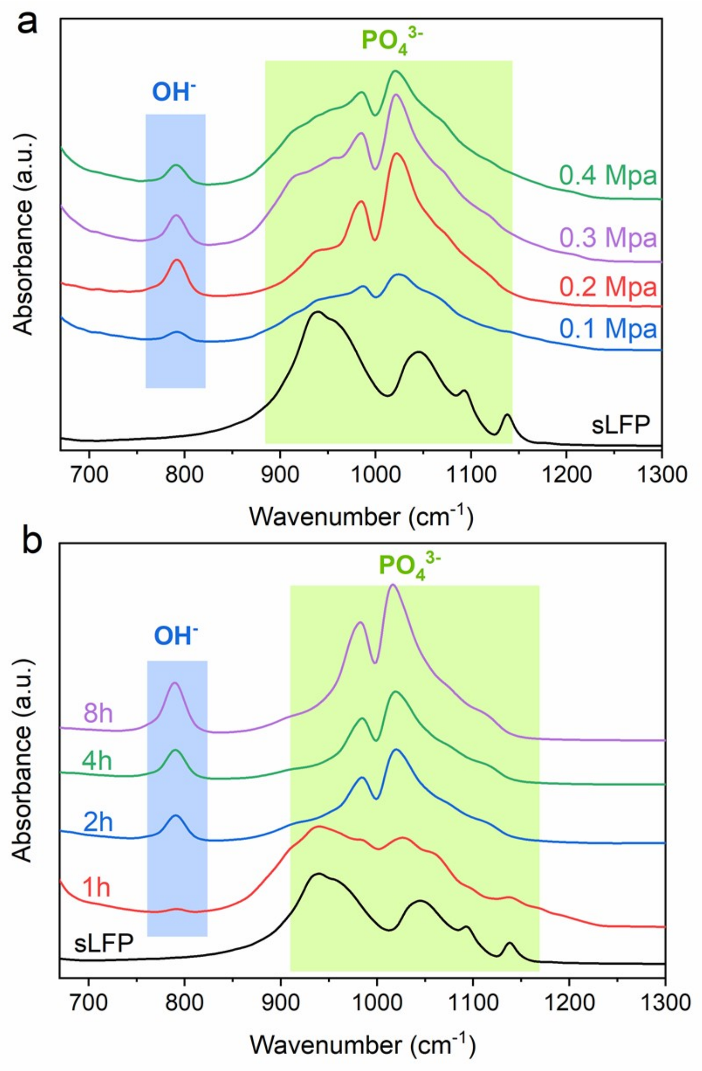

Figure S4. FT-IR spectrum of leaching residues under different (a) oxygen partial pressures (temperature: 210 °C; Leaching time: 2 h) and (b) leaching times (temperature: 210 °C; partial oxygen pressure: 0.3 MPa).

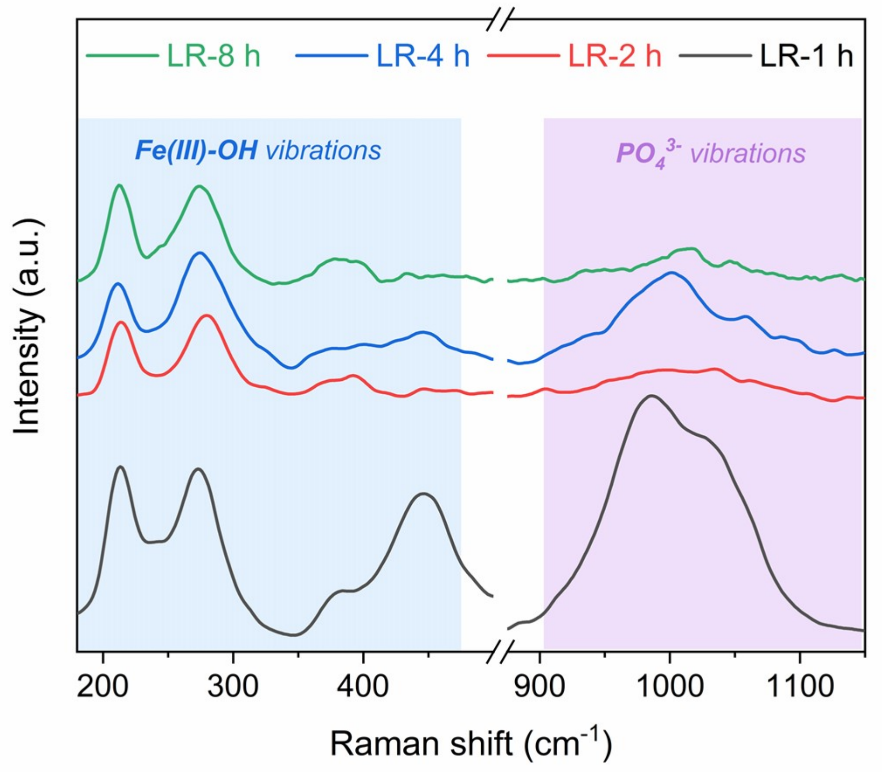

Figure S5. Raman spectra of leaching residues under different leaching times. (Temperature: 210 °C; partial oxygen pressure: 0.3 MPa)

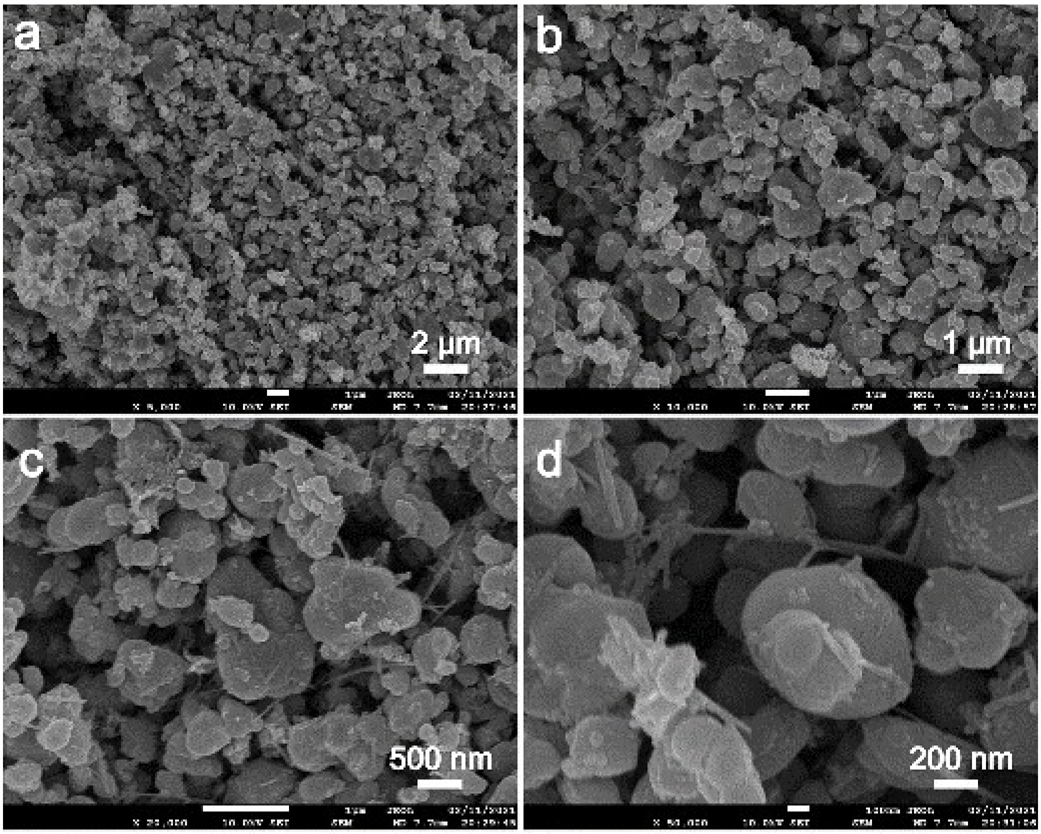

Figure S6. FESEM images of spent $LiFePO_4$ raw material.

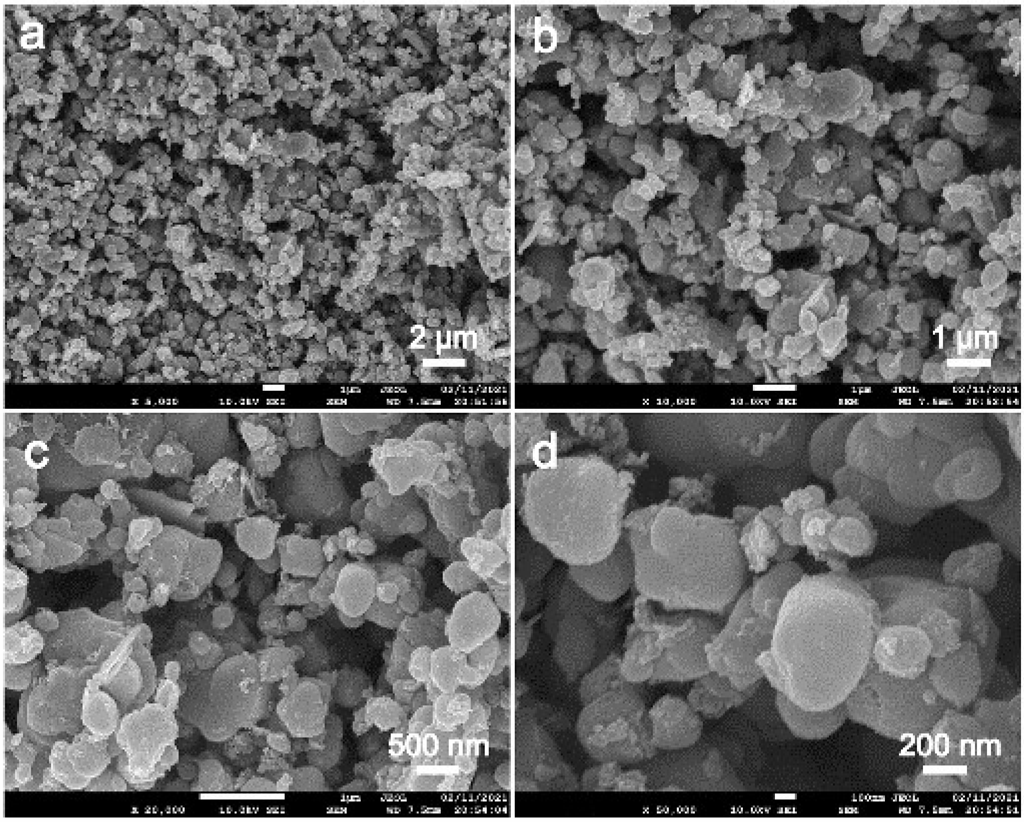

Figure S7. FESEM images of the LR-120 sample.

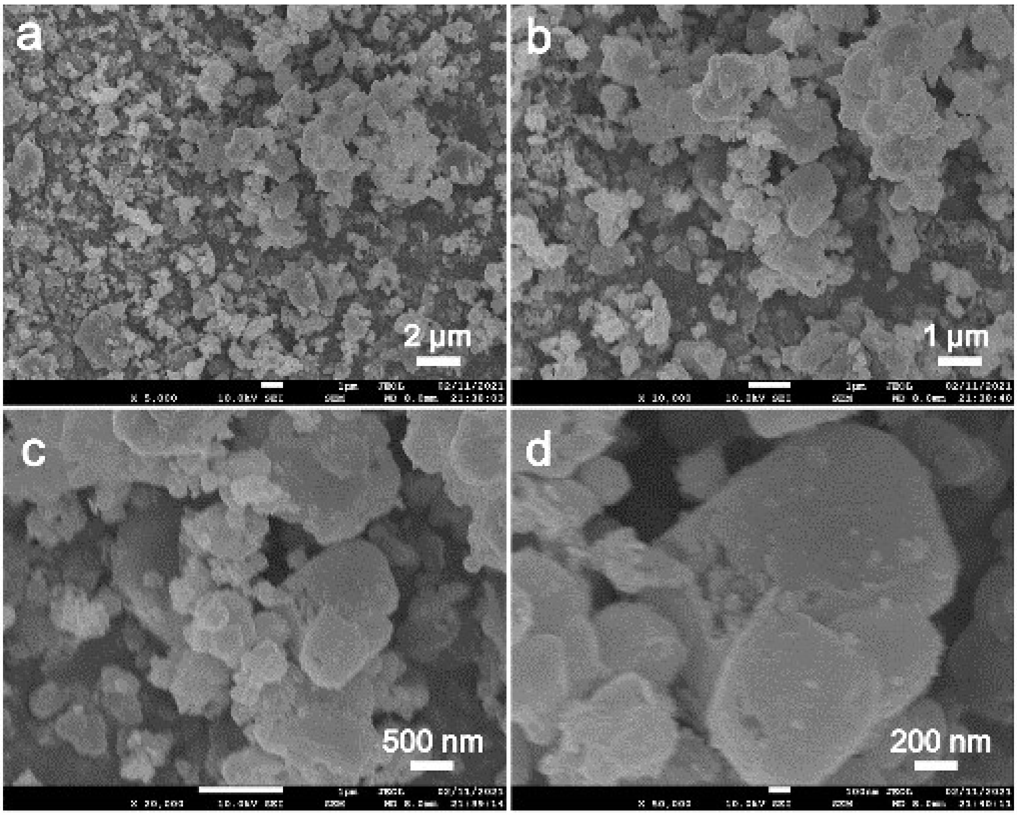

Figure S8. FESEM images of the LR-150 sample.

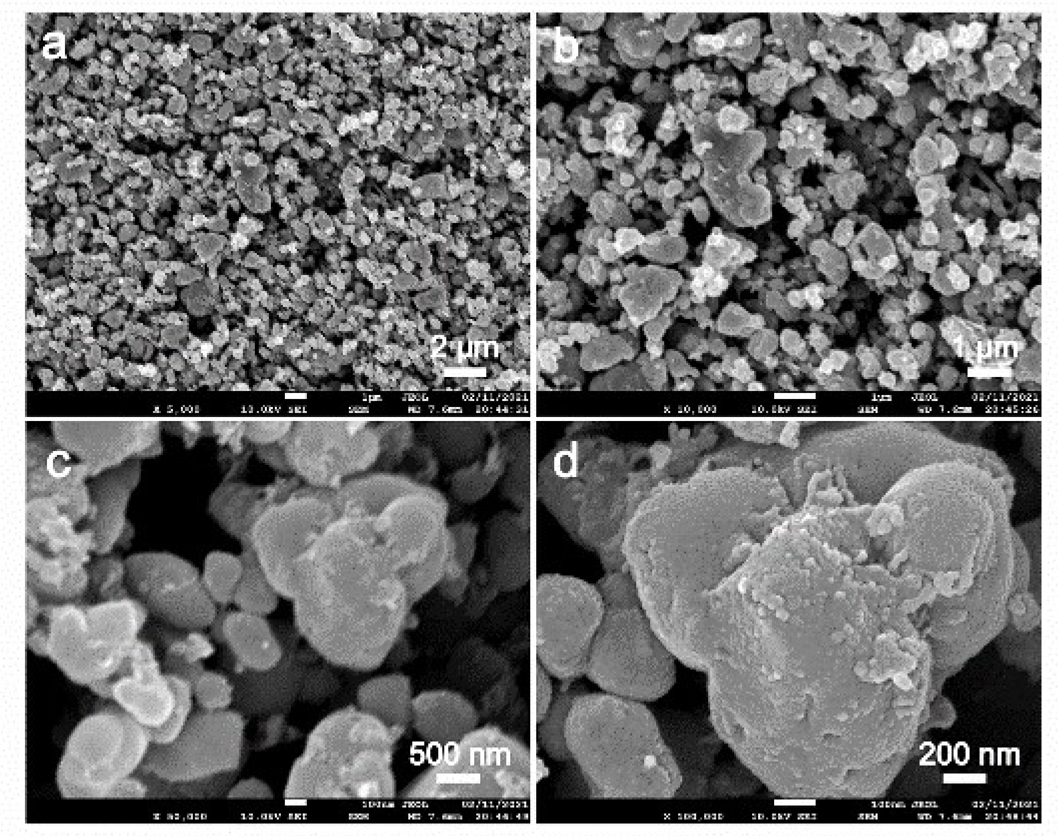

Figure S9. FESEM images of the LR-180 sample.

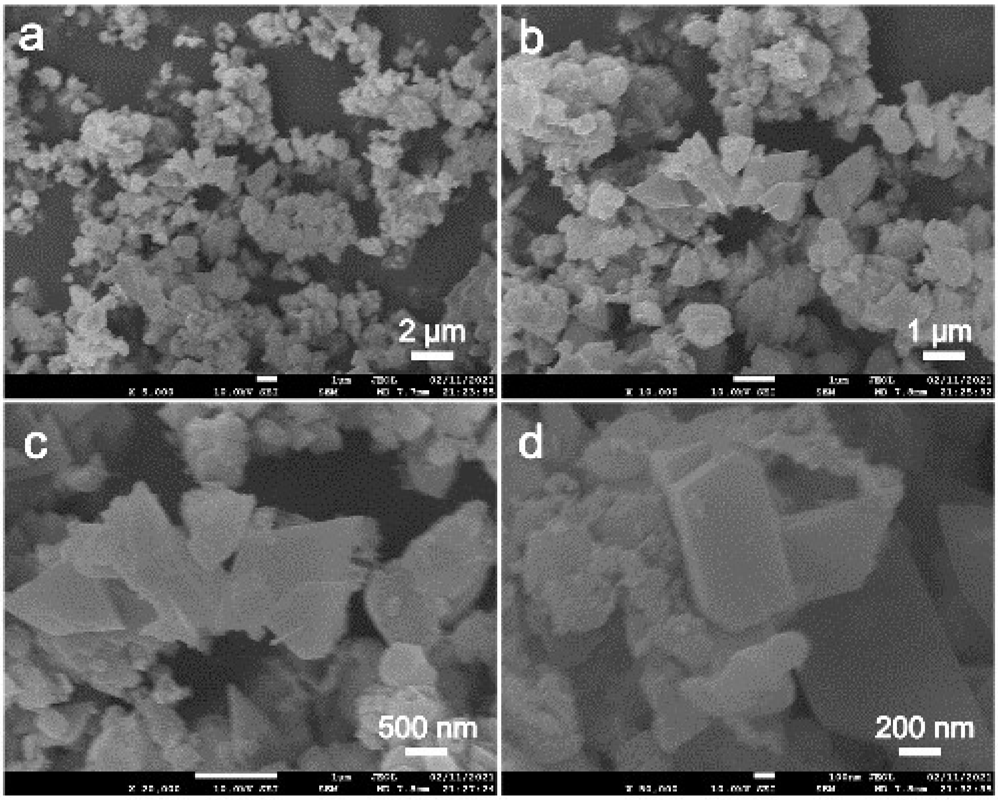

Figure S10. FESEM images of the LR-210 sample.

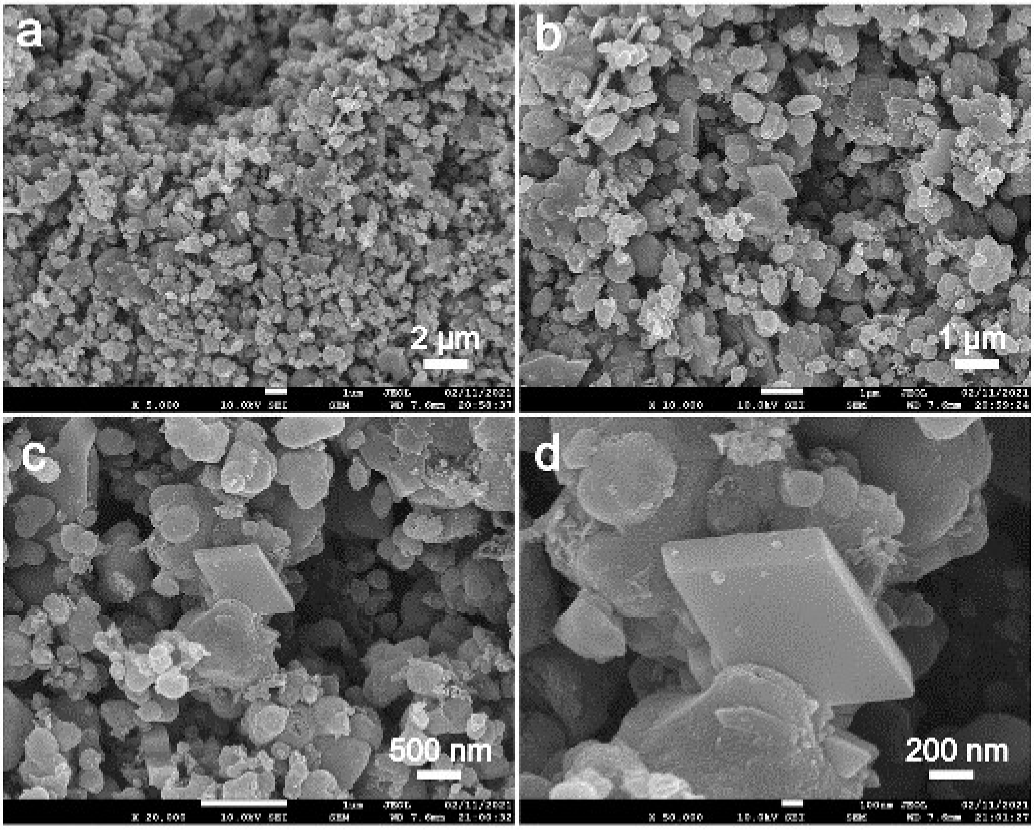

Figure S11. FESEM images of the LR-240 sample.

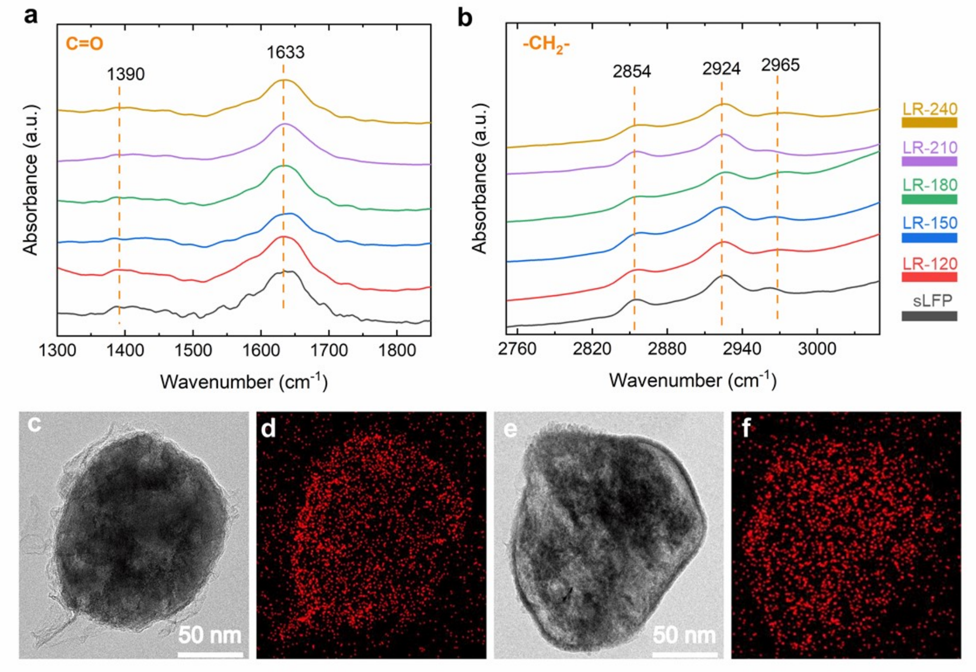

Figure S12. FT-IR spectra of sLFP and leaching residues under various temperatures in the wavenumber region of (a) 1300–1900 cm^{-1} and (b) 2750–3050 cm^{-1}; (c) TEM image and (d) EDS mapping of carbon element of the LR-120 sample; (e) TEM image and (f) EDS mapping of carbon element of the LR-210 sample.

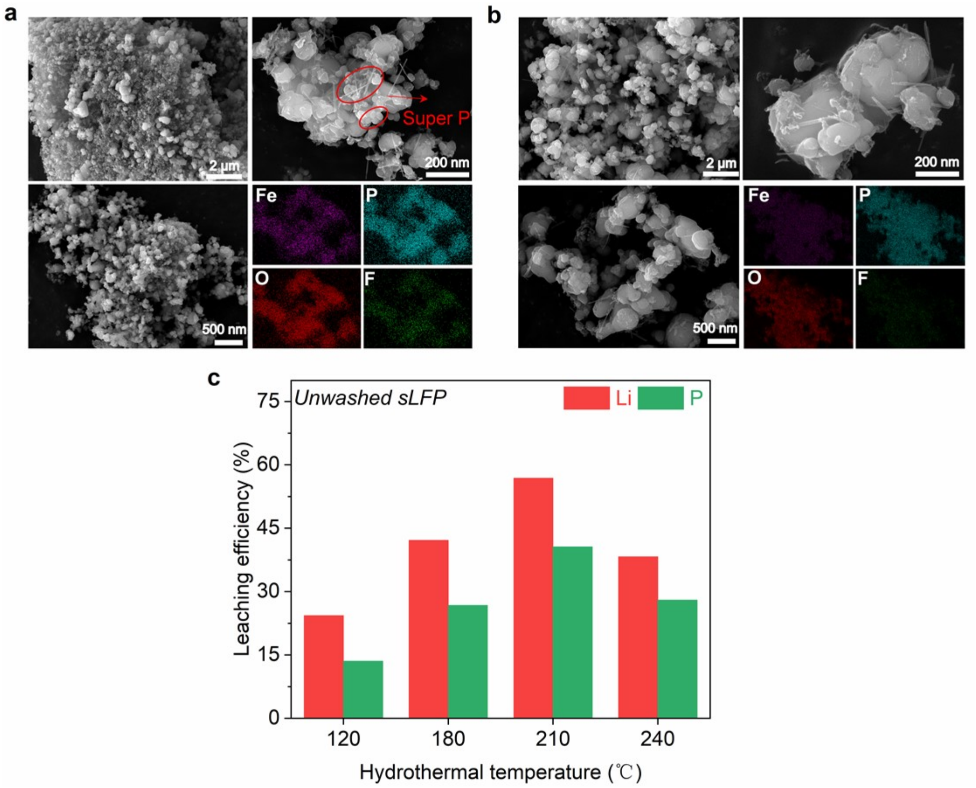

Figure S13. FESEM and EDS images of the sLFP powder (a) before NMP washing, and (b) after NMP washing; (c) Leaching efficiency of the Li and P elements of unwashed sLFP powder under various hydrothermal temperature (Oxygen partial pressure: 0.3 MPa; leaching time: 2 h).

In the unwashed sLFP sample, it could be observed that nano-sized Super P particles were attached around the sLFP particles, and the PVDF were also existed in the powders according to the EDS mapping images (**Fig. S13a**). As for the washed sample, the absence of F element in the EDS mapping images (**Fig. S13b**) demonstrated the successful removal of PVDF. Additionally, the spherical Super P was also disappeared around the sLFP particles. Considering the contact between PVDF/Super P with sLFP particles is loose and the contact area is small, they have little effect on the sLFP leaching, as confirmed in **Fig. S13c**.

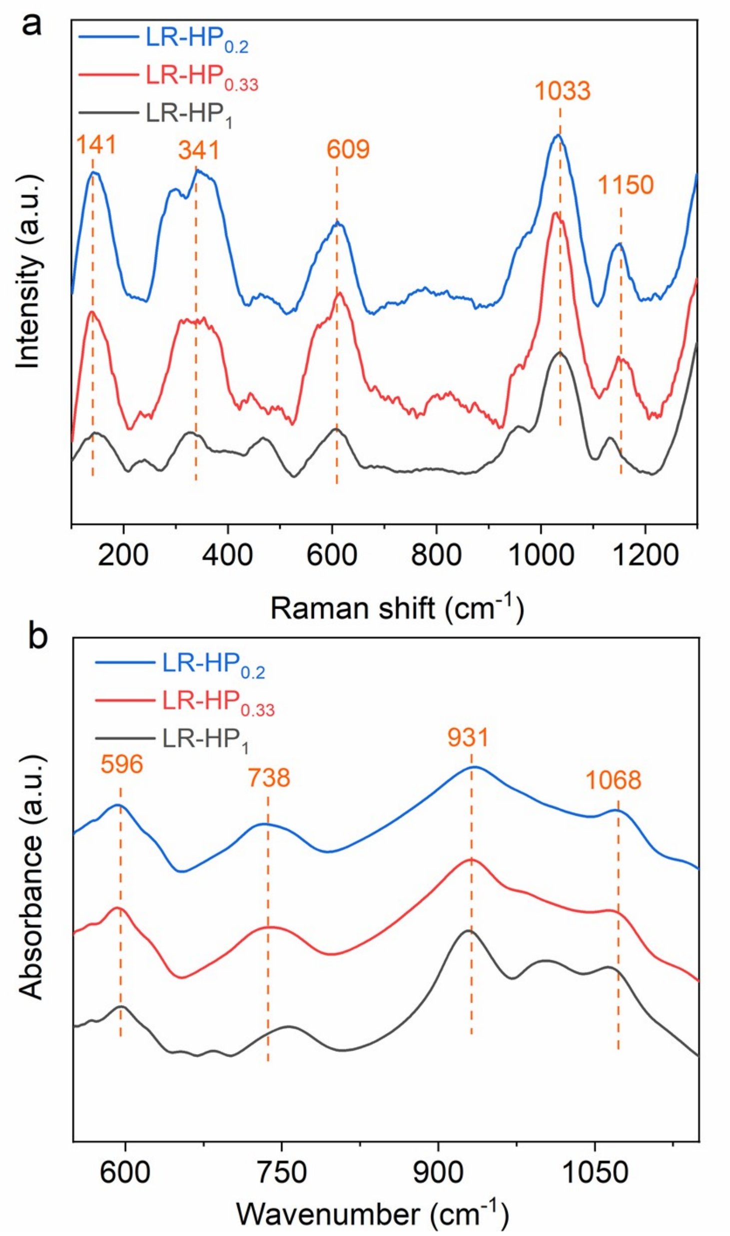

Figure S14. Raman and FT-IR spectra of obtained leaching residues with various H_3PO_4 supplied amounts.

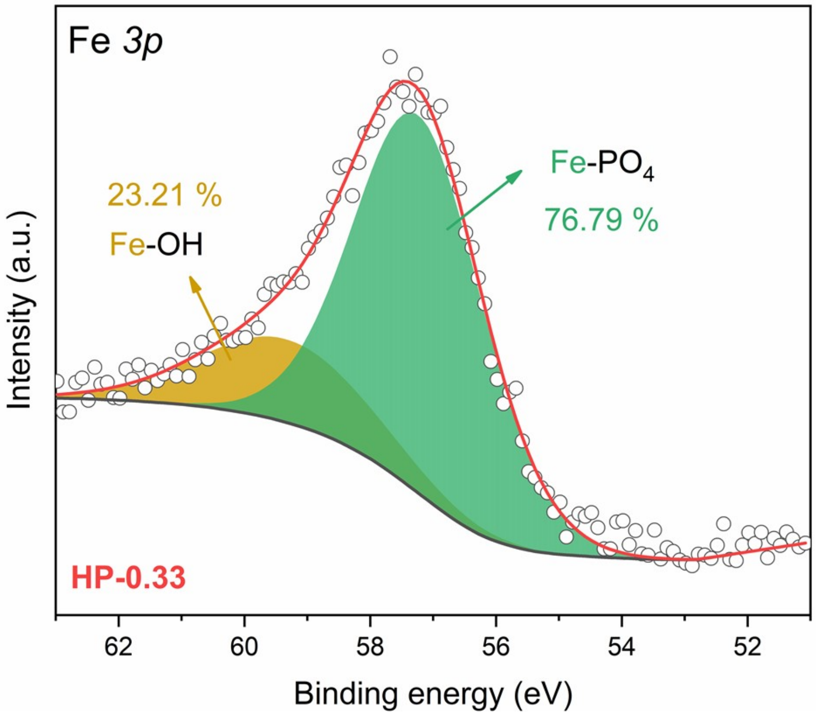

Figure S15. High-resolution XPS spectrum of Fe 3*p* orbital in LR-$HP_{0.33}$.

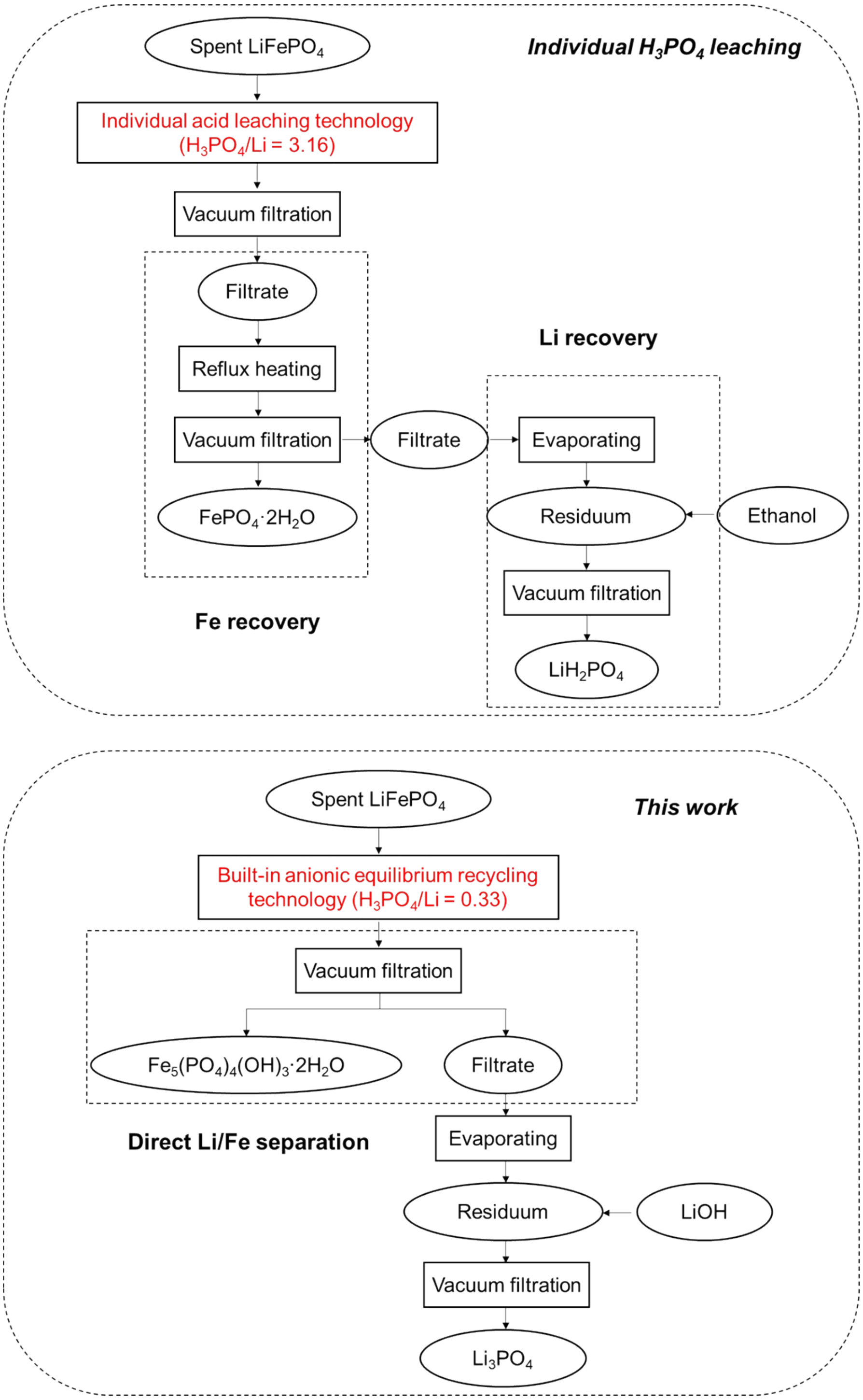

Figure S16. The flowchart comparison of the individual H_3PO_4 leaching process [1] and this proposed work.

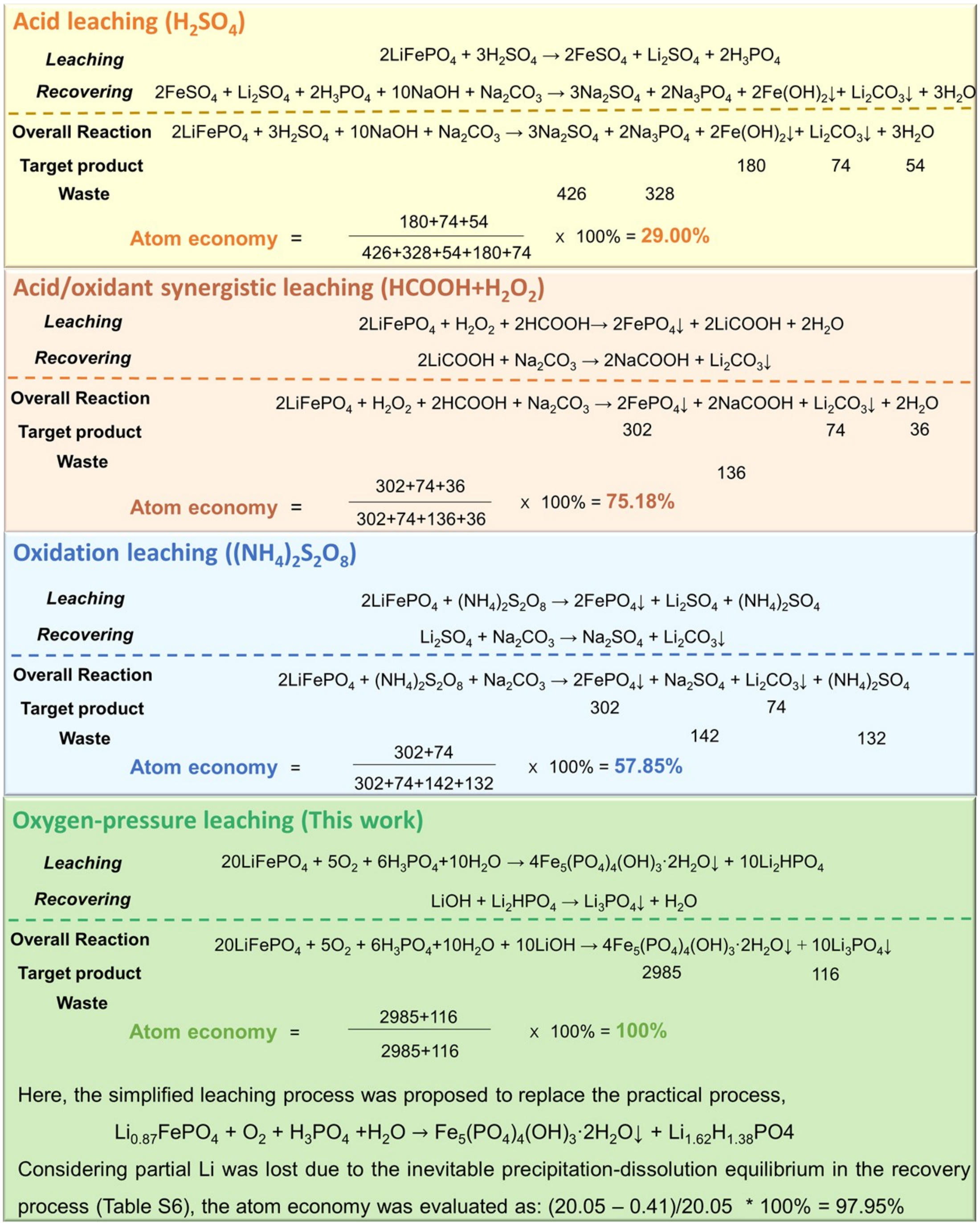

Acid leaching (H_2SO_4)

Leaching $2LiFePO_4 + 3H_2SO_4 \rightarrow 2FeSO_4 + Li_2SO_4 + 2H_3PO_4$

Recovering $2FeSO_4 + Li_2SO_4 + 2H_3PO_4 + 10NaOH + Na_2CO_3 \rightarrow 3Na_2SO_4 + 2Na_3PO_4 + 2Fe(OH)_2\downarrow + Li_2CO_3\downarrow + 3H_2O$

Overall Reaction $2LiFePO_4 + 3H_2SO_4 + 10NaOH + Na_2CO_3 \rightarrow 3Na_2SO_4 + 2Na_3PO_4 + 2Fe(OH)_2\downarrow + Li_2CO_3\downarrow + 3H_2O$

Target product 180 74 54

Waste 426 328

Atom economy $= \frac{180+74+54}{426+328+54+180+74} \times 100\% = 29.00\%$

Acid/oxidant synergistic leaching ($HCOOH+H_2O_2$)

Leaching $2LiFePO_4 + H_2O_2 + 2HCOOH \rightarrow 2FePO_4\downarrow + 2LiCOOH + 2H_2O$

Recovering $2LiCOOH + Na_2CO_3 \rightarrow 2NaCOOH + Li_2CO_3\downarrow$

Overall Reaction $2LiFePO_4 + H_2O_2 + 2HCOOH + Na_2CO_3 \rightarrow 2FePO_4\downarrow + 2NaCOOH + Li_2CO_3\downarrow + 2H_2O$

Target product 302 74 36

Waste 136

Atom economy $= \frac{302+74+36}{302+74+136+36} \times 100\% = 75.18\%$

Oxidation leaching ($(NH_4)_2S_2O_8$)

Leaching $2LiFePO_4 + (NH_4)_2S_2O_8 \rightarrow 2FePO_4\downarrow + Li_2SO_4 + (NH_4)_2SO_4$

Recovering $Li_2SO_4 + Na_2CO_3 \rightarrow Na_2SO_4 + Li_2CO_3\downarrow$

Overall Reaction $2LiFePO_4 + (NH_4)_2S_2O_8 + Na_2CO_3 \rightarrow 2FePO_4\downarrow + Na_2SO_4 + Li_2CO_3\downarrow + (NH_4)_2SO_4$

Target product 302 74

Waste 142 132

Atom economy $= \frac{302+74}{302+74+142+132} \times 100\% = 57.85\%$

Oxygen-pressure leaching (This work)

Leaching $20LiFePO_4 + 5O_2 + 6H_3PO_4 + 10H_2O \rightarrow 4Fe_5(PO_4)_4(OH)_3{\cdot}2H_2O\downarrow + 10Li_2HPO_4$

Recovering $LiOH + Li_2HPO_4 \rightarrow Li_3PO_4\downarrow + H_2O$

Overall Reaction $20LiFePO_4 + 5O_2 + 6H_3PO_4 + 10H_2O + 10LiOH \rightarrow 4Fe_5(PO_4)_4(OH)_3{\cdot}2H_2O\downarrow + 10Li_3PO_4\downarrow$

Target product 2985 116

Waste

Atom economy $= \frac{2985+116}{2985+116} \times 100\% = 100\%$

Here, the simplified leaching process was proposed to replace the practical process,

$Li_{0.87}FePO_4 + O_2 + H_3PO_4 + H_2O \rightarrow Fe_5(PO_4)_4(OH)_3{\cdot}2H_2O\downarrow + Li_{1.62}H_{1.38}PO4$

Considering partial Li was lost due to the inevitable precipitation-dissolution equilibrium in the recovery process (Table S6), the atom economy was evaluated as: (20.05 – 0.41)/20.05 * 100% = 97.95%

Figure S17. Leaching/recovering reactions and atom economy assessment in acid leaching (H_2SO_4) [2], acid/oxidant synergistic leaching ($HCOOH+H_2O_2$) [3], oxidation leaching ($(NH_4)_2S_2O_8$) [4] processes and this proposed work.

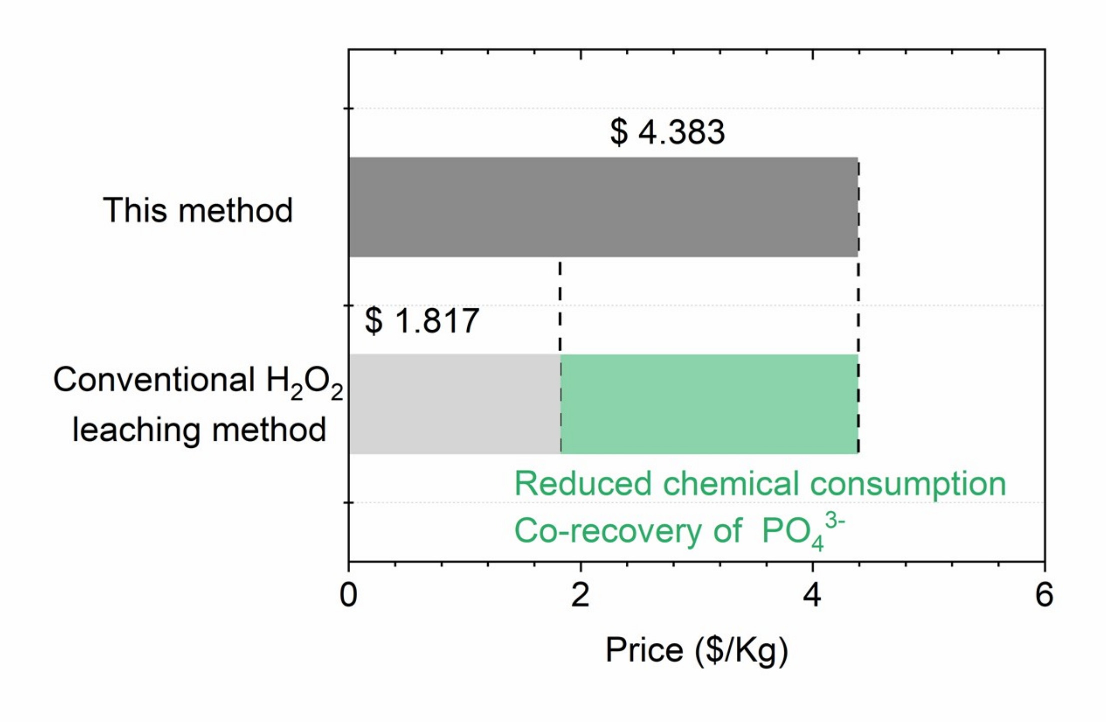

Figure S18. The profit of recycling sLFP with conventional H_2O_2 recycling method and proposed recycling method [5].

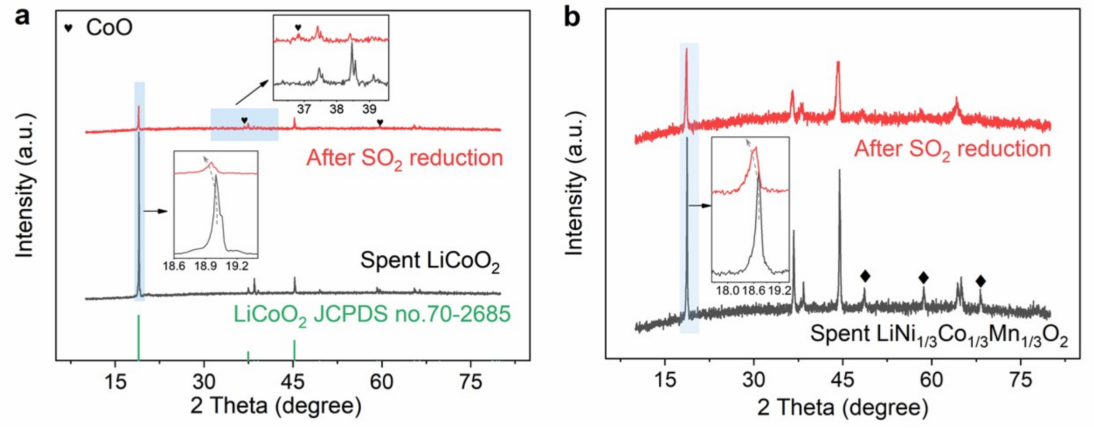

Figure S19. XRD patterns of (a) spent $LiCoO_2$ raw material and the leaching residue after SO_2 reduction, and (b) spent $LiNi_{1/3}Co_{1/3}Mn_{1/3}O_2$ raw material and the leaching residue after SO_2 reduction.

Based on the proposed built-in equilibrium methodology, some gas reductants (SO_2, CO) might be effective to achieve high atom economy for spent $LiCoO_2$ and $LiNi_xCo_yMn_zO_2$ ($x + y + z = 1$), as shown in equations S1 ~ S4:

SO_2 reductant:

$$SO_2 + 2LiCoO_2 \rightarrow Li_2SO_4 + 2CoO\downarrow \tag{S1}$$

$$SO_2 + 2LiNi_{1/3}Co_{1/3}Mn_{1/3}O_2 \rightarrow Li_2SO_4 + 2/3Ni_{1/3}Co_{1/3}Mn_{1/3}O\downarrow \tag{S2}$$

CO reductant:

$$CO + 2LiCoO_2 \rightarrow Li_2CO_3 + 2CoO\downarrow \tag{S3}$$

$$CO + 2LiNi_{1/3}Co_{1/3}Mn_{1/3}O_2 \rightarrow Li_2CO_3 + 2/3Ni_{1/3}Co_{1/3}Mn_{1/3}O\downarrow \tag{S4}$$

The feasibility study was conducted on spent $LiCoO_2$ and $LiNi_{1/3}Co_{1/3}Mn_{1/3}O_2$ cathodes under SO_2 atmosphere (hydrothermal temperature: 200 °C; SO_2 partial pressure: 0.3 MPa; leaching time: 3 h). Although not under optimal condition, the selective leaching of lithium can be achieved for spent $LiCoO_2$ and $LiNi_{1/3}Co_{1/3}Mn_{1/3}O_2$ with efficiency of 64.26% and 60.02%, respectively. As shown in the XRD patterns of the leaching residues (**Fig. S19**), it could be observed that all peak intensity was greatly decreased due to the leaching of raw material. The main diffraction peaks of both spent $LiCoO_2$ and $LiNi_{1/3}Co_{1/3}Mn_{1/3}O_2$ sample shifted to a smaller angle after reduction, indicating an expanded interplanar spacing based on the Bragg equation. As shown in the **Fig. S19a**, the peaks located at 36.8° and 59.7° could be assigned to the CoO phase. The disappeared diffraction peaks located at 48.7°, 58.6°, and 68.2° in reacted $LiNi_{1/3}Co_{1/3}Mn_{1/3}O_2$ sample also implied a phase transition after SO_2 reduction (**Fig. S19b**). Anyway, these results preliminarily confirmed the feasibility of the built-in equilibrium recycling strategy in spent $LiCoO_2$ and $LiNi_{1/3}Co_{1/3}Mn_{1/3}O_2$.

Table S1. ICP data of the leachates and calculated leaching efficiency of various elements.

Samples	Experimental variable	Conditions	Element concentration in leachates (mg L^{-1})*			Volume of leachates (mL)	Leaching efficiency (%)		
			Li	P	Fe		Li	P	Fe
Sample 1	Temperature (℃) (Oxygen partial pressure: 0.2 MPa; Leaching time: 2 h)	120	183.77	483.08	5.70	478	25.31	13.03	0.085
Sample 2		150	193.02	528.73	4.38	469	26.09	13.99	0.064
Sample 3		180	292.15	981.73	6.14	465	39.15	25.76	0.089
Sample 4		210	444.20	1631.30	2.91	452	57.86	41.61	0.041
Sample 5		240	295.05	1110.69	0.15	447	38.01	28.02	0.002
Sample 6	Oxygen partial pressure (MPa) (Temperature: 210 ℃; Leaching time: 2 h)	0.1	389.60	1325.86	5.40	451	50.64	33.75	0.076
Sample 7		0.2	455.11	1698.32	0.86	449	58.89	43.03	0.012
Sample 8		0.3	502.82	1735.58	6.23	453	65.64	44.37	0.088
Sample 9		0.4	503.66	1655.80	6.55	450	65.32	42.05	0.092
Sample 10	Leaching time (h) (Temperature: 210 ℃; Oxygen partial pressure: 0.3 MPa)	1	367.00	1361.12	3.44	475	50.24	36.49	0.051
Sample 11		2	501.46	1719.82	3.41	452	65.32	43.87	0.048
Sample 12		4	458.50	1688.61	5.77	439	58.01	41.83	0.079
Sample 13		6	395.57	1514.28	1.60	421	47.99	35.98	0.021
Sample 14		8	301.28	1149.13	0.97	398	34.56	25.81	0.012

*Note: Li and P contents in the leachate were analyzed after diluting for 50 times by 0.1 M HNO_3.

Table S2 Traditional band positions and shoulders of $Fe(OH)_3$, FeOOH and Fe_2O_3 in the region 200~1000 cm^{-1} reported in the literature [6, 7].

Crystalline phase	Band positions (cm^{-1})
α-FeOOH	205, 247, 300, 418, 481, 549
β-FeOOH	310, 390, 535, 610, 720
γ-FeOOH	400, 677
Fe_2O_3	226, 245, 292, 411, 497, 612

Table S3. ICP data of the obtained leachates with stoichiometric H_3PO_4 supplied.

Samples	Leachates	Element concentration in leachates (mg L^{-1})*			Volume of leachates (mL)	Leaching efficiency (%)		Li/P molar ratio
		Li	P	Fe		Li	Fe	
Sample 15	L-$HP_{0.2}$	457.86	1187.88	2.32	457	60.30	0.033	1.72
Sample 16	L-$HP_{0.33}$	697.04	1920.06	6.04	456	91.60	0.086	1.62
Sample 17	L-HP_1	717.40	4212.26	6.62	460	95.11	0.095	0.76

*Note: Li and P contents in the leachate were analyzed after diluting for 200 times by 0.1 M HNO_3.

Table S4. Distribution of Li and P elements in leachates and LRs based on Li conservation.

n (H_3PO_4/Li)	Content/mol (Leachates)		Content/mol (Residues)			P content/mol	
	Li	P	Li	P		Theoretical	Calculated
			Li_3PO_4	Li_3PO_4	FPOH		
0.20	0.60	0.33	0.40	0.13	0.80	1.20	1.26
0.33	0.92	0.47	0.08	0.03	~0.80	1.33	1.30
1.00	0.95	0.99	0.05	0.02	0.80	2.00	1.81

Noted: Assuming the LFP is 1 mol.

Table S5. The calculation of the P leaching efficiency from the sLFP.

Leachates	Measured P concentration (mg L^{-1})	Added P from H_3PO_4 (mg L^{-1})	Leaching from sLFP (mg L^{-1})	Leaching efficiency (%)
L-$HP_{0.2}$	5.9394	3.3888	2.5506	13.156
L-$HP_{0.33}$	9.6003	5.6038	3.9965	20.569
L-HP_1	21.0613	16.8302	4.2311	21.967

Table S6. Elements concentrations, solution volume, and solution pH before and after Li_3PO_4 recovery.

Samples	Elements concentration (g L^{-1})			Solution volume (mL)	Solution pH
	Li	P	Fe		
In the L-$HP_{0.33}$	0.697	1.920	0.006	456	2.45
After concentrated	20.05	55.21	0.17	16	1.23
After Li recovery	0.41	0.92	0.01	32	8.01

Based on the Li and P elements concentrations in the concentrated leachates, the content of the $Li_{1.62}H_{1.38}PO_4$ was evaluated as 28.53 mmol. The added LiOH was calculated as 1.5 mol L^{-1} * 27 mL = 40.50 mmol. The precipitation reaction between $Li_{1.62}H_{1.38}PO_4$ and LiOH could be depicted as follow:

$$Li_{1.62}H_{1.38}PO_4 + 1.38\ LiOH \rightarrow Li_3PO_4\downarrow + 1.38\ H_2O$$

According to the precipitation reaction, 39.37 mmol of LiOH is required to completely convert the soluble $Li_{1.62}H_{1.38}PO_4$ as Li_3PO_4 precipitate. Thus, 1.13 mmol LiOH was superfluous and left in the solution. The residue Li content after Li_3PO_4 recovery was evaluated as 1.84 mmol according to the detected Li concentration (0.41 g L^{-1}). The loss Li content (from sLFP) in the recovery process could be calculated as: (1.84 – 1.13)/46.22 *100% = 1.54 %. Thus, the Li recovery efficiency from the initial sLFP could be calculated as: 91.6% * (1 - 1.54 %) = 90.19%. Similarly, the P recovery efficiency from sLFP is calculated as: 20.57% * (1 – 3.33 %) = 19.88%.

Notably, because distilled water (~425 mL) was collected during the concentrated process, the residual mother liquor and distilled water could be further recycled.

Table S7. Performance of common leaching agents for Li extraction from spent LFP cathode materials.

Process	Reagents	Conditions			Leaching Efficiency (%)		Ref.
		Concentration (usage)	Temperature and time	s/L (g/L)	Li	Fe	
Acid leaching	H_2SO_4	H_2SO_4/$LiFePO_4$ = 8 (molar ratio)	60 °C/none	/			8
	MSA + H_2O_2	MSA: 8 mol/L; H_2O_2: 18 vol%	25 °C + 1.5 h	80	94	95	9
	TsOH + H_2O_2	MSA: 4 mol/L; H_2O_2: 18 vol%	25 °C + 1.5 h	60	81	78	9
	H_2SO_4	2 mol/L	70 °C + 2 h	50	96.67	93.25	10
	H_2SO_4	2.5 mol/L	Pyrometallurgy (600 °C + 1 h); 60 °C +4 h.	100	97	98	11
	H_3PO_4	0.5 mol/L	25 °C + 1 h; Reflux heating (85 °C + 9 h).	25	>95	/	1
Acid/oxidant synergistic leaching	CH_3COOH+H_2O_2 (30 wt.%)	CH_3COOH: 0.8 mol/L; H_2O_2: 6 vol%	50 °C + 0.5 h	120	95.05	/	12
	H_2SO_4 +H_2O_2	H_2SO_4/Li = 0.57 (molar ratio); H_2O_2/Li = 2.07 (molar ratio)	60 °C + 2 h	90	96.85	0.03	13

	H_2SO_4 +$Na_2S_2O_8$	H_2SO_4: 0.3 mol/L; $Na_2S_2O_8$/Li = 0.45 (molar ratio)	60 °C + 1.5h	90	97.55	1.39	[14]
	HCOOH + H_2O_2 (30 wt.%)	HCOOH: 0.4 mol/L; H_2O_2:3 vol%	60 °C + 1/3 h	50	98.84	<1	[3]
Oxidizing leaching	$Fe_2(SO_4)_3$	$Fe_2(SO_4)_3$/Li = 0.57 (molar ratio)	28 °C + 0.5 h	500	97.07	/	[15]
	$Na_2S_2O_8$	$Na_2S_2O_8$/Li = 0.53 (molar ratio)	25 °C +1/3 h	300	99.9	0.048	[16]
	$(NH_4)_2S_2O_8$	$(NH_4)_2S_2O_8$/Li = 0.7 (molar ratio)	30 °C + 0.5 h	50	97.7	<1	[4]
	$Na_2S_2O_8$	$Na_2S_2O_8$/Li = 0.7 (molar ratio)	25 °C + 0.5 h	50	~100	/	[17]
	$K_2S_2O_8$	$K_2S_2O_8$/Li = 0.5 (molar ratio)	/	/	/	/	[18]

Noted: Density of 30 wt.% H_2O_2 at 25 °C is 1.11 g mL^{-1};

MSA: Methane sulfonic acid, CH_3SO_3H;

TsOH: p-toluenesulfonic acid, $CH_3C_6H_4SO_3H$.

Economic analysis (Table S8)

Taking 1.0 ton of spent $LiFePO_4$ cathode as example, an industrial economic analysis is processed. To preferably perform the economic advantages of proposed recycling method, profits is calculated based on the inputs and outputs. The details are showed as follow:

Table S8. The reagents and energy consumption to dispose 1 ton of spent $LiFePO_4$ cathode in our work [4, 5, 10, 19].

	Items	Price	Dosage	Cost
Leaching	Water (H_2O)	$\$/\text{m}^3$	m^3	$\$$
		0.65	50	32.50
	Phosphoric acid (H_3PO_4)	$\$/\text{t}$	t	$\$$
		1272.44	0.33	419.91
	Oxygen (O_2)	$\$/\text{m}^3$	m^3	$\$$
		42.41	5.00	212.05
	Energy cost	$\$/\text{kW h}$	kW h	$\$$
		0.129	3000.00	387.00
Recovering	Lithium hydroxide (LiOH)	$\$/\text{t}$	t	$\$$
		43121.73	0.08	3449.74
	Energy cost	$\$/\text{kW h}$	kW h	$\$$
		0.129	500.00	64.50
Total				4565.7 $\$$

Inputs:

(1) The cost of raw materials is calculated as follows: Spent $LiFePO_4$ battery is 5250 $\$$/ton. Therefore, the input cost of 1.0 ton of spent $LiFePO_4$ cathode is calculated

as 14660 \$ (Considering the 35.8% cathode content in spent batteries) [4, 5].

Spent $LiFePO_4$ cathode:

14660 \$/t × 1.00 t = 14660.00 \$

(2) The cost of reagents for the leaching and recovering process is calculated as below:

H_2O:

0.65 \$/m^3 × 50.00 m^3 = 32.50 \$

H_3PO_4 **(Sources:** http://www.100ppi.com/mprice/plist-1-6774-1.html, accessed May 29, 2023, ¥ 7.073 = 1 \$**)**:

1272.44 \$/t × 0.33 t = 419.91 \$

O_2 **(Sources:** https://www.1688.com, accessed May 29, 2023, ¥ 7.073 = 1 \$**):**

42.41 \$/m^3 × 5.00 m^3 = 212.05 \$

LiOH (Sources: http://www.100ppi.com/vane/detail-1239.html, accessed May 29, 2023, ¥ 7.073 = 1 \$):

43121.73 \$/t × 0.08 t = 3449.74 \$

(3) The **energy consumption** cost of entire processes is calculated as follow:

Leaching process: 0.129 \$/kW h × 3000.00 kW h = 387.00 \$

Recovering process: 0.129 \$/kW h × 500.00 kW h = 64.50 \$

(4) Labor (200 \$/t) (**Sources:** https://doi.org/10.1016/j.seppur.2023.123742)

200 \$/t × 1.00 t = 200.00 \$

Inputs were calculated as 19425.70 \$.

Outputs:

(1) The outputs for recycling process were from the recovering of 0.29 ton of Li_3PO_4

(Scale up from laboratory) regardless of obtained FPOH.

Li_3PO_4 **(Sources:** https://doi.org/10.1016/j.seppur.2023.123742**):**

82100 $/t × 0.29 t = 23809.01 $

Profits:

The ultimate profits are calculated as:

23809.01 $ - 19425.70 $ = 4383.31 $

Table S9. Mass fractions of the Li, Fe, and P elements, and calculated Fe/Li and Fe/P molar ratios in the sLFP.

Elements	Li	Fe	P
Mass fraction in sLFP (wt%)	3.47	32.05	17.72
Mass in 100 g of sLFP (g)	3.47	32.05	17.72
Molar mass (g mol^{-1})	6.94	55.85	30.97
Amount of substance (mol)	0.499	0.574	0.57

The elemental molar ratios of the Fe/Li and Fe/P were calculated as 0.871 and 1.003, respectively, indicating the average composition of $Li_{0.87}FePO_4$ in the sLFP powder.

Table S10. The specific H_3PO_4 adding amounts (mass, amount of substance, and concentration) in the H3PO4-suppleid experiments.

Experiments	H_3PO_4/Li = 0.2	H_3PO_4/Li = 0.33	H_3PO_4/Li = 1.0
Mass of sLFP powder (g)	10.00	10.00	10.00
Amount of substance of contained Li (mmol)	49.99	49.99	49.99
Amount of substance of added H_3PO_4 (mmol)	10.00	16.50	49.99
Mass of added H_3PO_4 (g)	1.15	1.90	5.76
H_3PO_4 concentration (mol L^{-1})	0.02	0.033	0.100

Note: The solution volume is 500 mL; the mass fraction of the H_3PO_4 reagent is 85%.

References

1. D. C. Bian, Y. H. Sun, S. Li, Y. Tian, Z. H. Yang, X. M. Fan and W. X. Zhang, *Electrochim. Acta*, 2016, **190**, 134-140.
2. Y. Wu, K. Zhou, X. Zhang, C. Peng, Y. Jiang and W. Chen, *Waste Manage.*, 2022, **144**, 303-312.
3. G. J. Ji, X. Ou, R. R. Zhao, J. F. Zhang, J. T. Zou, P. F. Li, D. Z. Peng, L. Ye, B. Zhang and D. He, *Resources Conservation and Recycling*, 2021, **174**, 105802.
4. D. Z. Peng, J. F. Zhang, J. T. Zou, G. J. Ji, L. Ye, D. M. Li, B. Zhang and X. Ou, *J. Clean Prod.*, 2021, **316**, 128098.
5. H. Zhou, Z. Luo, S. Wang, X. Ma and Z. Cao, *Sep. Purif. Technol.*, 2023, **315**, 123742.
6. M. K. Nieuwoudt, J. D. Comins and I. Cukrowski, *J. Raman Spectrosc.*, 2011, **42**, 1335-1339.
7. D. L. A. de Faria, S. Venâncio Silva and M. T. de Oliveira, *J. Raman Spectrosc.*, 1997, **28**, 873-878.
8. G. Q. Cai, K. Y. Fung, K. M. Ng and C. Wibowo, *Ind. Eng. Chem. Res.*, 2014, **53**, 18245-18259.
9. P. Yadav, C. J. Jie, S. Tan and M. Srinivasan, *J. Hazard. Mater.*, 2020, **399**, 123068.
10. Y. F. Song, B. Y. Xie, S. L. Song, S. Y. Lei, W. Sun, R. Xu and Y. Yang, *Green Chem.*, 2021, **23**, 3963-3971.
11. R. J. Zheng, L. Zhao, W. H. Wang, Y. L. Liu, Q. X. Ma, D. Y. Mu, R. H. Li and C. S. Dai, *RSC Adv.*, 2016, **6**, 43613-43625.
12. Y. X. Yang, X. Q. Meng, H. B. Cao, X. Lin, C. M. Liu, Y. Sun, Y. Zhang and Z. Sun, *Green Chem.*, 2018, **20**, 3121-3133.
13. H. Li, S. Z. Xing, Y. Liu, F. J. Li, H. Guo and G. Kuang, *ACS Sustain. Chem. Eng.*, 2017, **5**, 8017-8024.
14. H. Y. Li, H. Ye, M. C. Sun and W. J. Chen, *J. Cent. South Univ.*, 2020, **27**, 3239-3248.
15. Y. Dai, Z. Xu, D. Hua, H. Gu and N. Wang, *J. Hazard. Mater.*, 2020, **396**, 122707.
16. J. L. Zhang, J. T. Hu, Y. B. Liu, Q. K. Jing, C. Yang, Y. Q. Chen and C. Y. Wang, *ACS Sustain. Chem. Eng.*, 2019, **7**, 5626-5631.
17. X. H. Yue, C. C. Zhang, W. B. Zhang, Y. F. Wang and F. S. Zhang, *Chem. Eng. J.*, 2021, **426**, 131311.
18. B. Gangaja, S. Nair and D. Santhanagopalan, *ACS Sustain. Chem. Eng.*, 2021, **9**, 4711-4721.
19. X. J. Qiu, B. C. Zhang, Y. L. Xu, J. G. Hu, W. T. Deng, G. Q. Zou, H. S. Hou, Y. Yang, W. Sun, Y. H. Hu, X. Y. Cao and X. B. Ji, *Green Chem.*, 2022, **24**, 2506-2515.